PROCEEDINGS, 41st Workshop on Geothermal Reservoir Engineering
Stanford University, Stanford, California, February 22-24, 2016
SGP-TR-209

Numerical Modeling of the Stimulation Program at RRG-9 ST1, a DOE EGS

Jacob Bradford[1], John McLennan[1], Joseph Moore[2], Robert Podgorney[3], Greg Nash[2], Mary Mann[4], William Rickard[4], and Douglas Glaspey[5]

[1]Department of Chemical Engineering, University of Utah, Salt Lake City, UT, 84112, USA

[2]Energy & Geoscience Institute at the University of Utah, Salt Lake City, UT, 84108, USA

[3]Idaho National Laboratory, Idaho Falls, ID, 83415, USA

[4]Geothermal Resource Group, Inc., Palm Desert, CA, 92211, USA

[5]US Geothermal Inc., 1505 Tyrell Lane, Boise, ID 83706, USA

J.T.Bradford@utah.edu

Keywords: enhanced geothermal system, hydraulic fracturing, thermal fracturing, Raft River

ABSTRACT

The Raft River geothermal field is the location of a Department of Energy (DOE) enhanced geothermal system test site. The field is located roughly 161 km (100 miles) northwest of Salt Lake City on the Utah Idaho border. Since 2012, the test well RRG-9 ST1 has been successfully stimulated hydraulically and thermally. The well was initially hydraulically stimulated using flow rates from 42 to 2,877 Lpm (11 to 760 gpm) at an injection pressure of 7,924 kPa (1,150 psi). The well was then shut in to allow for the construction of a 254 mm (10 inch) pipeline from the plant to the wellhead. In 2013, injection from the plant through the 254 mm (10 inch) line was initiated at a flow rate of 76 Lpm (20 gpm) at an injection pressure of about 1,937 kPa (280 psi). A second hydraulic stimulation utilizing an agricultural pump raised flow rates into the well to 643 Lpm (170 gpm). Flow rates were further increased to 1,249 Lpm (330 gpm) with the addition of a second pump. Following this second stimulation, injection was resumed through the 254 mm (10 inch) pipeline and injection improved from 189 to 454 Lpm (50 gpm to 120 gpm). Injection was maintained through the winter of 2013 and spring of 2014 when a third hydraulic stimulation was performed on the well in April 2014. Using pump trucks, a maximum flow rate of 4,769 Lpm (1,260 gpm) was achieved at an injection pressure of 6,752 kPa (980 psi). Following this hydraulic stimulation, injection was resumed into the pipeline. The injectivity of the well has steadily improved since the third stimulation. In April 2015 a pressure falloff test at the well led to further increases in well injectivity. Currently the well accepts 3,785 Lpm (1,000 gpm) at an injection pressure of 1,550 kPa (225 psi). The injectivity of the well has improved from 0.08 Lpm/kPa to 2.4 Lpm/kPa (0.15 gpm/psi to 4.4 gpm/psi) during the course of the stimulation program.

Microeismic events related to plant activity have been monitored through an eight-station microseismic array deployed around the RRG-9 ST1 wellhead. Since 2010 over 180 microseismic events have been recorded. The majority of these events follow a linear trend to the northeast of the RRG-9 ST1 wellhead. This trend corresponds to the location of the Narrows shear zone. The presence of these events indicates that fluid injected into RRG-9 ST1 travels along this zone to the northeast. Additionally, a correlation between the frequency of microseismic events and increases in the injectivity of the well has been found. Prior to each major increase in injectivity, an enhanced number of microseismic events are detected.

The RRG-9 ST1 stimulation program has been numerically modeled using FALCON a finite element reservoir simulation code developed by the Idaho National Laboratory. This model uses a continuum approach to simulate fluid flow through the fracture networks surrounding RRG-9 ST1. The permeability of these fracture zones is adjusted to correspond to the increasing injectivity of the well. The timing of these permeability adjustments are tied to the occurrence of increased numbers of microseismic events. Using this method, a pressure history match has been obtained for the RRG-9 ST1 stimulation program.

1. INTRODUCTION

The Raft River geothermal field is located 161 km (100 miles) northwest of Salt Lake City and is the site of a Department of Energy Enhanced Geothermal System (EGS) project. Four injection wells (RRG-3, 6, 9 ST1, and 11) and four production wells (RRG-1, 2, 4, and 7) have been drilled into the Precambrian rocks that host the geothermal reservoir Figure 1).

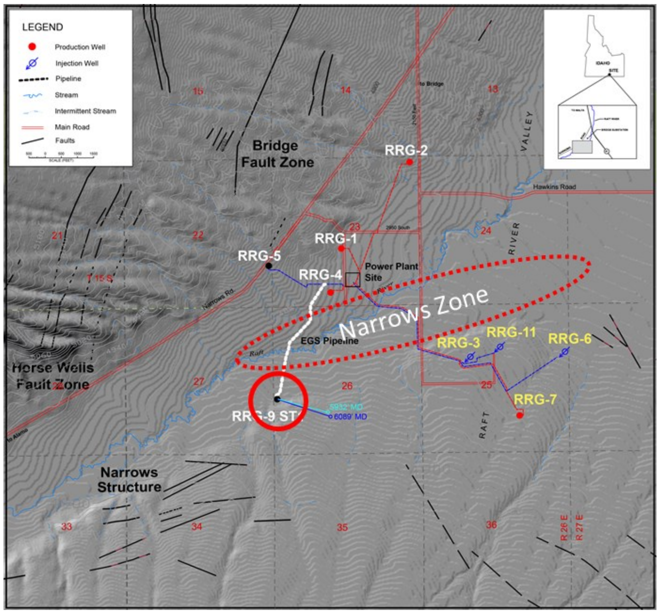

Figure 1: Geology of the Raft River geothermal field. Fault locations based on Williams et al. (1982). Production wells include RRG-1, 2, 4, and 7 while RRG-3, 6, 9 ST1, and 11 are used as injection wells. RRG-5 is no longer in use as an injection well. RRG-9 ST1 is circled in red. The approximate location of the Narrows Zone is shown by the dotted red line. The presence of the Narrows Zone was based on geochemical data as discussed in the text Ayling and Moore (2013).

RRG-9 ST1 was originally drilled to explore the southwest extension of the high temperature fracture found in RRG-7. In February 2012 the well was sidetracked and deepened to a depth of 1,808 m MD (5,932 ft.). The well penetrated 183 m (680 ft.) of the Elba quartzite, the primary reservoir formation. The well was cased to approximately 1,686 m (5,532 ft.) leaving 121 m (400 ft.) of open-hole below the casing. Since 2012 the injection well RRG-9 ST1 has been hydraulically and thermally stimulated to create an enhanced geothermal system.

The geology of Raft River field is complex (see for example Konstantinou (2012) and Nash and Moore (2012)). Geologic studies, water chemistry, microseismic monitoring, and borehole imaging have been used to develop a conceptual model of the Raft River geothermal reservoir. Production and injection wells pass through roughly 1,524 m (5,000 ft.) of discontinuous Quaternary and Tertiary volcanic and volcanoclastic rocks before entering the Precambrian metamorphic basement. The chemical data show that wells in the northern part of the field have lower salinities than those in the southeast although all of the wells are drilled into the same Precambrian basement rocks. Ayling and Moore (2013) concluded that the two portions of the field are separated by a low permeability barrier that they termed the Narrows Zone (Figure 1). To the southwest of the Narrows Zone, faults strike northeast-southwest. North of the Narrows Zone, faults strike to the north-south. To the east, faults strike northwest.

Locally generated microseismic events attributed to the stimulation program show a linear trend of events extending northeast from the RRG-9 ST1, parallel to the inferred location of the Narrows Zone. We suggest that the presence of these microseismic events reflect fluid movement along the Narrows Zone. Image logs and temperature data demonstrate that water injected into RRG-9 ST1 exits the well through a fracture in the Precambrian Elba quartzite between 1,719 to 1,725 m MD (5,640 to 5,660 ft.). This fracture strikes northeast-southwest and is steeply dipping. This fracture when projected to the northeast will intersect the Narrows Zone approximately 1 km from the wellhead. There is no direct evidence that any of the other 82 fractures in the open-hole section of the well 1,684 to 1,804 m MD (5,524.59 ft. to 5,920.8 ft.) have accepted appreciable amounts of injectate. Figure 2 is a conceptual model of the geothermal system based on these data.

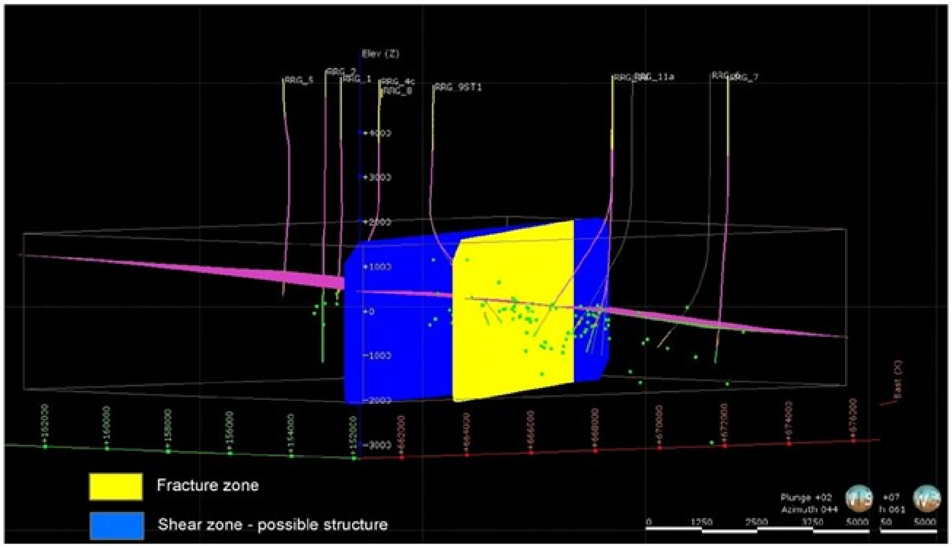

Figure 2: Raft River conceptual model. The pink plane denotes the Tertiary-Precambrian contact. The blue plane is the Narrows Zone, and the yellow plane is the fracture identified at 1,719 to 1,725 m MD (5,640 to 5,660 ft.).

In this model fluid injected into the RRG-9 ST1 passes through the fracture located at 1,719 to 1,725 m MD (5,640 to 5,660 ft.) which connects into the Narrows Zone. The injected water then moves along the Narrows Zone to the northeast.

2. STIMULATION PROGRAM

RRG-9 ST1 was hydraulically stimulated in February 2012. Since it was initially unknown how much fluid the well would accept, flow rates were increased in a step wise fashion from 42 to 2,877 Lpm (11 to 760 gpm) at a maximum pressure of 7,924 kPa (1,150 psi). Following the hydraulic stimulation, the well was shut in for a year and a half while the 254 mm (10 inch) pipeline was constructed from the plant to RRG-9 ST1 and environmental reviews were completed. In June, 2013 nearly continuous injection of water from the plant, through the pipeline was initiated. Initial injection rates were less than 76 Lpm (20 gpm) at a wellhead pressure of 1,929 kPa (280 psi). A second hydraulic stimulation using agricultural pumps to increase flow rates was conducted during August and September, 2013. Flow rates of up to 1,249 Lpm (330 gpm) were achieved during this time period. As a result of the second hydraulic stimulation, flow rates increased from 189 to 454 Lpm (50 to 120 gpm). Injection continued through winter and spring of 2014 when a third hydraulic stimulation was conducted in April 2014. During the third hydraulic stimulation flow rates up to 4,769 Lpm (1,260 gpm) at a wellhead pressure of 6,752 kPa (980 psi) where achieved. Following the third stimulation injection was resumed. Further discussion of the hydraulic stimulations of RRG-9 ST1 is given in Bradford et al. (2015). After the third stimulation, the well began to steadily accept water at increasing flow rates up to 2,082 Lpm (550 gpm) in April of 2015. It had been observed that shutting in the other injection wells for a short time period improved their injectivity. This method was applied to RRG-9 ST1 in April/June, 2015 and again in August, 2015. When injection was resumed, the rate of increase in injectivity was greater than before the well was shut-in. Injection has continued into RRG-9 ST1 from the plant and is currently at a rate of 3,785 Lpm (1,000 gpm) at a wellhead pressure of 1,557 kPa (226 psi). The stimulation program at RRG-9 ST1 is summarized in Table 1.

Table 1 RRG-9 ST1 Stimulation Program.

Date	Stimulation Phase
February 2012	First Hydraulic Stimulation
June 2013 to August 2013	Injection of plant water through the 254 mm (10 inch) pipeline begins.
August/September 2013	Second Hydraulic Stimulation
September 2013 to April 2014	Injection of plant water through the 254 mm (10 inch) pipeline resumed.
April 2014	Third Hydraulic Stimulation
April 2014 to April 2015	Injection of plant water through the 254 mm (10 inch) pipeline resumed.
April 2015	RRG-9 ST1 shut-in.
April 2015 to August 2015	Injection of plant water through the 254 mm (10 inch) pipeline resumed.
August 2015	RRG-9 ST1 shut-in
August 2015 to Present	Injection of plant water through the 254 mm (10 inch) pipeline resumed.

The flow rate, wellhead pressure and wellhead temperature have been monitored continuously since the stimulation program at RRG-9 ST1 began. A modified Hall plot of the stimulation program was constructed by plotting the cumulative bottom-hole flowing pressure versus the cumulative volume of fluid injected (Figure 3).

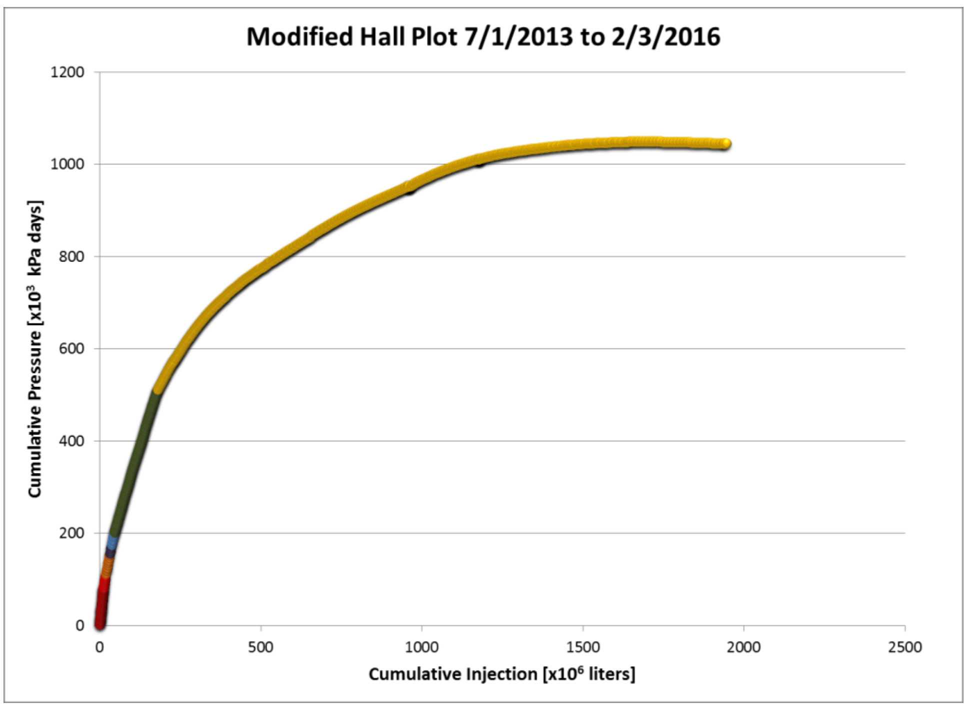

Figure 3: RRG-9 ST1 modified Hall plot. The decreasing slope of the line indicates that the skin factor is decreasing and/or the permeability is increasing as a result of the stimulation program.

The slope of the modified Hall plot is proportional to the change in the skin factor and inversely proportional to the reservoir permeability (Earlougher 1977). The decreasing slope indicates the skin factor has decreased around the well and/or that the permeability of the reservoir has improved. The improvements in permeability are attributed to both hydraulic and thermal opening of fractures near the wellbore and in the Narrows Zone.

3. MICROSEISMIC ACTIVITY

Local microseismic activity has been monitored since 2010. Over 185 locally generated events have been recorded by an eight station microseismic array deployed around RRG-9 ST1. These events range from -1.25 to 1.01 in magnitude. The majority of these events follow a linear trend that corresponds to the location of Narrows's Zone (Figure 4).

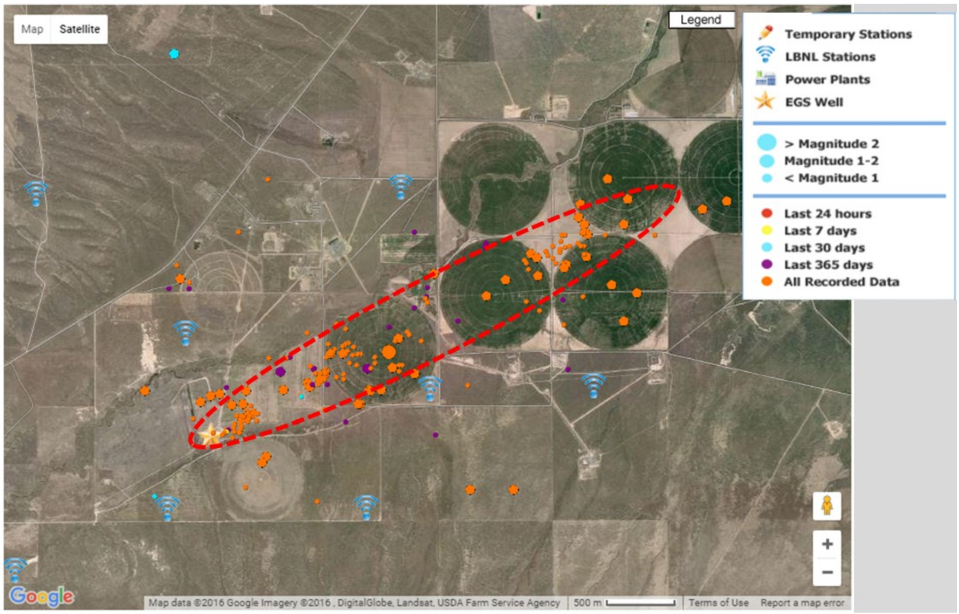

Figure 4: Microseismic activity at Raft River. The RRG-9 ST1 wellhead is shown as an orange star in the diagram. The red dashed line denotes the location of the Narrows Zone. The majority of microseismic events fall within this zone. The blue signal symbols are the location of the microseismic array stations. Image courtesy of Lawrence Berkley Laboratory.

The majority of these recorded events occurred in the Precambrian basement. The timing of microseismic events correlates with improvements in the injectivity of RRG-9 ST1. After the third stimulation, periods of increased microseismic activity, usually 6 to 10 microseismic events during the course of a single day, preceded positive changes in the injectivity of the well (Figure 5).

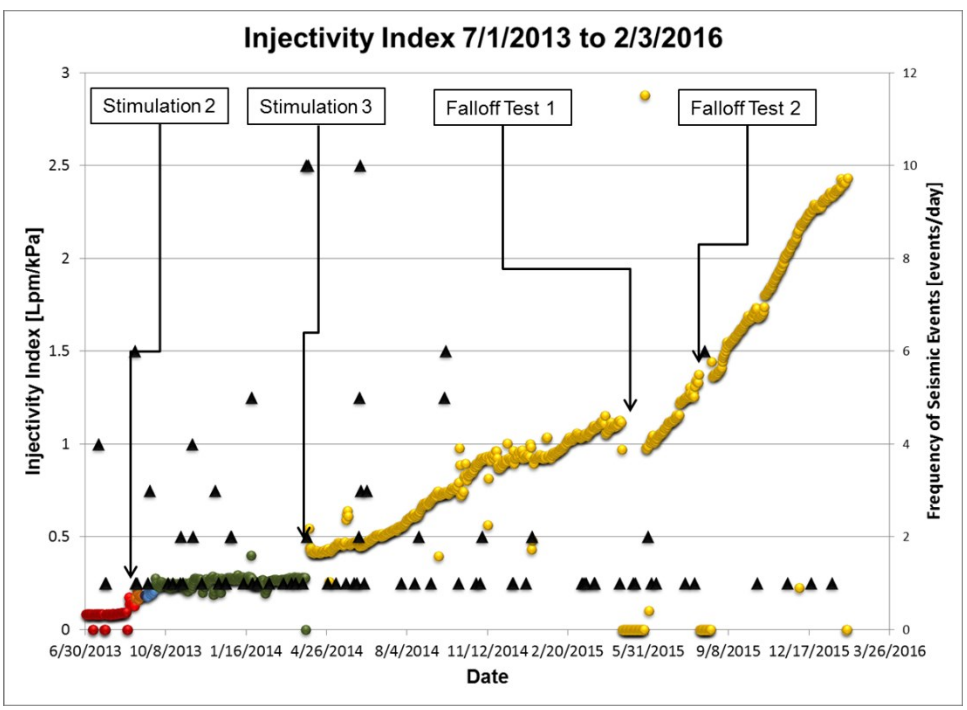

Figure 5: Injectivity index plot for RRG-9 correlated with the frequency of locally generated microseismic events. The injectivity index is plotted on the left hand axis as multicolored circles. Microseismic events (events per day) are plotted as black triangles on the right hand axis.

These periods of enhanced microseismic activity were mapped to determine their proximity to each other (Figure 6).

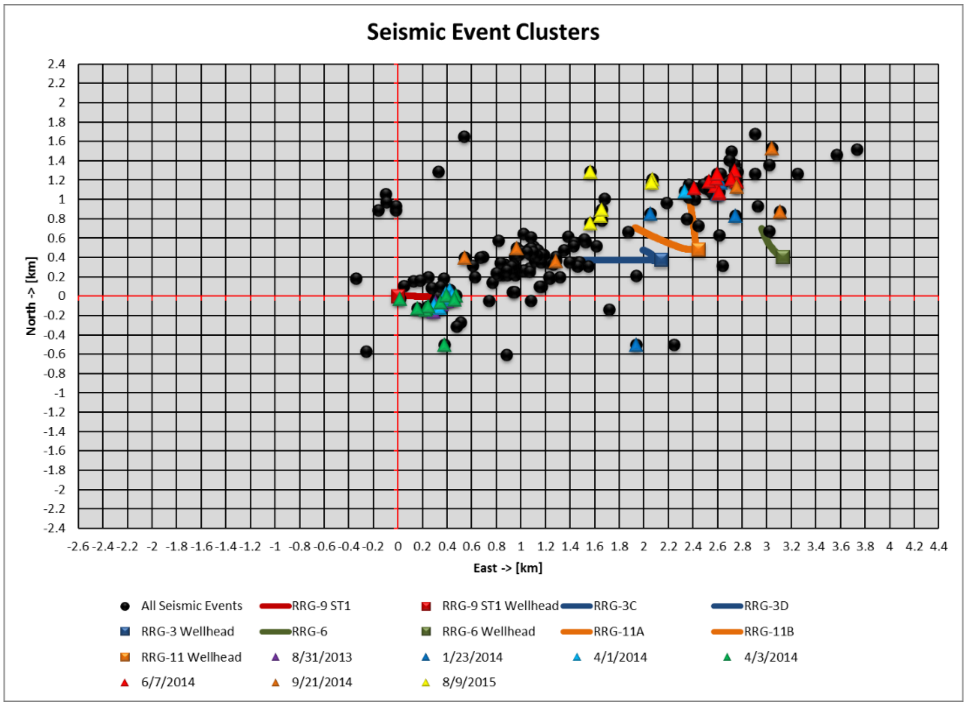

Figure 6: Map of microseismic event clusters. All distances are relative to the RRG-9 ST1 wellhead. Black circles denote the location of microseismic events. Multicolored triangles denote the various event clusters. The multicolored lines and squares represent the injection well trajectories and their respective wellhead locations relative to the RRG-9 ST1 wellhead.

The map of microseismic event clusters display an overall movement of events along the Narrows Zone to the northeast.

4. NUMERICAL MODELING

The stimulation program has been numerically modeled using FALCON, a finite element reservoir simulator developed by Idaho National Laboratory (Smith et al., 2013). The model developed for the RRG-9 ST1 stimulation program consists of a 10 by 10 km section of the reservoir centered on the RRG-9 ST1 wellhead. The fracture identified at 1,719 to 1,725 m MD (5,640 to 5,660 ft.) and the Narrows Zone are included in the model (Figure 7).

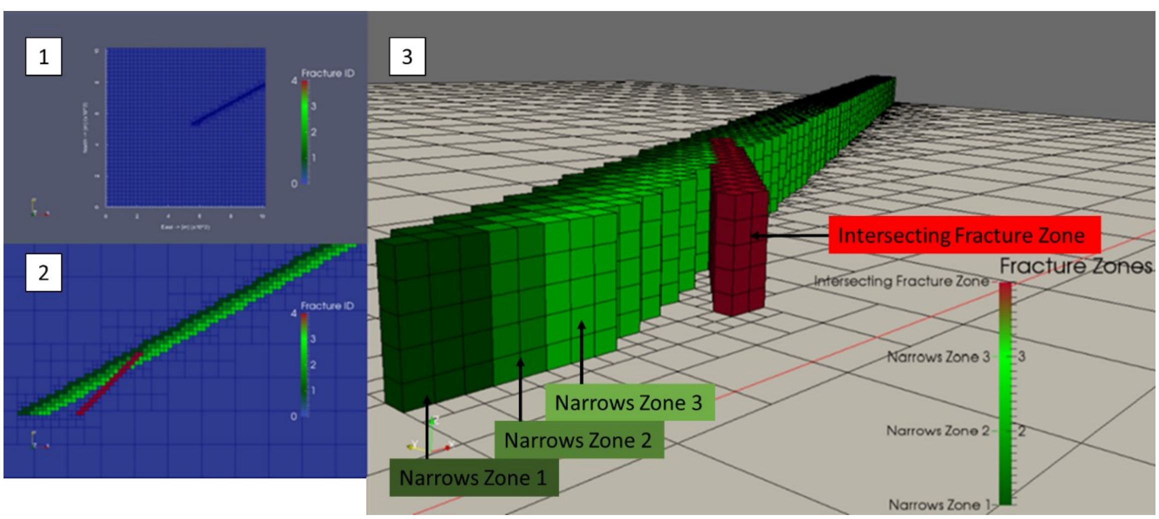

Figure 7: Model used in the simulation. 1: A top down view of the entire model. 2: A close up of the intersection of the fracture (red) and the Narrows Zone (green). 3: Three dimensional view of the intersecting fracture (red) and Narrows Zone (green). The rock matrix is shown in blue. The impermeable edge of the Narrows Zone fault core is the northwest edge of Narrows Zone 1 which borders the rock matrix.

FALCON uses a continuum approach to model fractures. Elements within the model containing either the fracture or the Narrows Zone are assigned a higher permeability value than the surrounding rock matrix. The Narrows Zone was divided up into three separate sections and assigned progressively smaller permeability values from northwest to southeast. Faults sometimes contain an impermeable core surrounded by fractures, the number of which decreases rapidly as one moves away from the fault core (Brogi, 2008). This was represented in the Narrows Zone through decreasing the permeability from Narrows Zone 1 to Narrows Zone 3. Using the flow rate data a pressure history match was obtained by adjusting the permeability of the fracture and the Narrows Zone. The timing and location of these permeability adjustments was based on the microseismic event clusters. Other adjustments were made to reflect aperture changes due to thermal cooling or other near wellbore effects. These adjustments are summarized in Table 2.

Table 2 Permeability Adjustments

Date	Adjustment Location	Fracture Zone Permeability [md]	Narrows Zone 1 Permeability [md]	Narrows Zone 2 Permeability [md]	Narrows Zone 3 Permeability [md]
Initial	Both	2.03E+00	1.01E+03	1.01E+02	1.01E+01
8/21/2013	Fracture Zone	3.04E+00	1.01E+03	1.01E+02	1.01E+01
8/31/2013	Fracture Zone	3.65E+00	1.01E+03	1.01E+02	1.01E+01
9/25/2013	Fracture Zone	7.09E+00	1.01E+03	1.01E+02	1.01E+01
1/23/2014	Narrows Zone	7.09E+00	1.01E+03	1.01E+02	1.01E+01
4/1/2014	Fracture Zone	1.52E+01	1.01E+03	1.01E+02	1.01E+01
4/3/2014	Fracture Zone	1.52E+01	1.01E+03	1.01E+02	1.01E+01
6/7/2014	Narrows Zone	1.52E+01	4.05E+03	4.05E+02	4.05E+01
9/21/2014	Narrows Zone	1.52E+01	8.11E+03	8.11E+02	8.11E+01
10/8/2014	Fracture Zone	2.03E+01	8.11E+03	8.11E+02	8.11E+01
1/6/2015	Fracture Zone	2.53E+01	8.11E+03	8.11E+02	8.11E+01
4/29/2015	Fracture Zone	3.04E+01	8.11E+03	8.11E+02	8.11E+01
8/3/2015	Fracture Zone	4.05E+01	8.11E+03	8.11E+02	8.11E+01
8/9/2015	Narrows Zone	4.05E+01	1.32E+04	1.32E+03	1.32E+02

The pressure history match obtained by adjusting the permeability is shown in Figure 8.

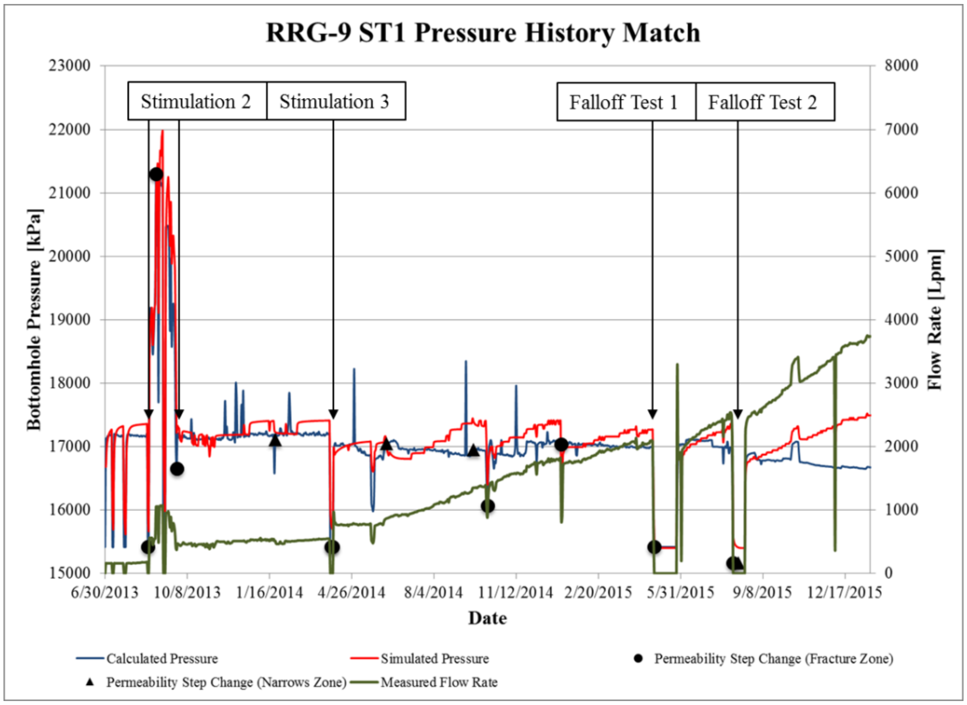

Figure 8: RRG-9 ST1 pressure history match. The blue line is the calculated bottomhole pressure in RRG-9 ST1. The red line is the simulated bottomhole pressure from FALCON. The green line is the injection flow rate. The black circles indicate step changes in permeability made to the fracture while the black triangles are the step changes in permeability made to the Narrows Zone.

The simulated pressure matches the calculated pressure quite well for the first third of the stimulation program. However, after the third hydraulic stimulation in April 2014, the calculated and measured cannot be reconciled. It is hypothesized that the nearly continuous cooling of the fractures has led to continuous increases in permeability due to thermal contraction of the rocks surrounding the fractures. These effects become more pronounced after the third hydraulic stimulation.

CONCLUSIONS

RRG-9 ST1 has been successfully hydraulically and thermally stimulated, which has led to flow rates increasing from 76 to 3,785 Lpm (20 gpm to1,000 gpm). The injectivity of the well has improved from 0.08 Lpm/kPa in July, 2013 to 2.4 Lpm/kPa in February, 2016 (0.15 gpm/psi to 4.4 gpm/psi). Geologic studies, water chemistry, microseismic monitoring, and borehole imaging suggest that the change in injectivity over time can be modeled by varying the permeability of a simple fracture network. This network consists of the fracture encountered in the well at depth of 1,719 to 1,725 m MD and the northeast trending Narrows Zone. The Narrows Zone acts as a conduit for fluids moving from the injection wells to the northeast while serving as barrier to fluid communication between the northwest and southeast portions of the field.

Analysis of flow rate and pressure data indicates the nearly continuous improvement in injectivity interpreted to result from a decrease in the skin factor and/or an increase in permeability. Although there is evidence of hydraulic and thermal effects the relative lack of microseismic activity implies that thermal effects predominate. Bottomhole pressures can be reasonably well matched by increasing the permeability of the fracture and the Narrows Zone through the early stimulations. These stimulations resulted in relatively minor increases in injectivity. In contrast injectivities increased rapidly and continuously after the high rate, high volume April 2014 stimulation, but bottomhole pressures remain relatively stable. In this case, simply increasing permeabilities based on microseismic activity does not lead to a reasonable pressure history match. These results suggest that thermal effects must be explicitly modeled. RRG-9 ST1 is a successful EGS project and the well is now in commercial use at the Raft River geothermal plant.

ACKNOWLEDGEMENTS

The authors are grateful to the management and staff of U.S. Geothermal Inc. and the DOE Technical Monitoring Team for their helpful comments and suggestions thought the course of this project. This work was funded under DOE Grant DE-FG36-08GO18189.

REFERENCES

Ayling, B., and Moore, J.N.: Fluid geochemistry at the Raft River geothermal field, Idaho, USA: New data and hydrogeological implications: Geothermics, v. 47, p. 116-126. (2013).

Bradford, J., Moore, J., Ohren, M., McLennan, J., Osborn, W., Majer, E., Nash, G., Podgorney, R., Freifeld, B., Nye, R., Rickard, W., waters, D., Glaspey, D.: Recent Thermal and Hydraulic Stimulation Results at Raft River, ID EGS Site: Proceedings, Fourtieth Workshop on Geothermal Reservoir Engineering, p. 561-571, (2015).

Brogi, A.: Fault zone architecture and permeability features in silicious sedimentary rocks: Insights from the Rapolano geothermal area (Northern Apennines, Italy), Journal of Structural Geology, pp. 237-256, (2008).

Earlougher JR., R.C.: Advances in Well Test Analysis, Dallas, TX (1977).

Konstantinou, A., Strickland, A., Miller, E. L., and Wooden, J. P.: Multistage Cenozoic extension of the Albion-Raft River-Grouse Creek metamorphic core complex: Geochronologic and stratigraphic constraints, Geosphere, v. 8, no. 6, p. 1429-1466. (2012).

Lawrence Berkeley Induced Seismicity: EGS: Interactive, Map of Earthquakes at Raft River. February 9, 2015. http://esd.lbl.gov/research/projects/induced_seismicity/egs/raft_river.html (accessed February 9, 2016).

Nash, G.D., Moore, J.N.: Raft River EGS project: a GIS-centric review of geology: GRC Transactions, v. 36, p. 951-958. (2012)

Smith K., Plummer, M., Bradford, J., and Podgorney, R., 2013. Adaptive mesh Refinement and Time Stepping Strategies for Incorporating Discrete Fracture Networks into a High Performance Computing framework for Geothermal Reservoir Simulation. GRC Transactions, v. 37 p. 857-862, (2013).

Williams, P.P., Covington, H.R. and Pierce, K.L.: Cenozoic stratigraphy and tectonic evolution of the Raft River basin, Idaho, in Cenozoic Geology of Idaho: Idaho Bureau of Mines and Geology Bulletin, v. 26, p. 491-504. Edited by Bonnichsen, B., and Breckenridge, R.M. (1982).